Design of a Model of Liquid Feeder to an Incinerator of Hazardous Waste and its Optimization from the Cooling Point of View: Part II

Ivan Mihálik[1*], Marián Lázár[2], Tomáš Brestovič[3], Peter Milenovský[4]

Department of Energy Engineering, Faculty of Mechanical Engineering, Technical University of Košice, Vysokoškolská 4, 042 00 Košice, Slovakia
*Corresponding Author

Received: 03 November 2023/ Revised: 15 November 2023/ Accepted: 21 November 2023/ Published: 30-11-2023

Abstract— *A series of articles aimed at the cooling of the liquid radioactive waste feeder into the incinerator space optimization. The second part examines ion-exchange resins used in the nuclear industry and the possibilities of their combustion. A 3D model of a radioactive waste feeder with different variants of cooling pipes is proposed. Using numerical simulation, the cooling efficiency of individual variants is compared.*

Keywords— ***Radioactive Waste, Ion-Exchange Resin, CFD Simulation, Heat Transfer, Cooling Optimization.***

I. INTRODUCTION

The first part of the article discussed individual types of radioactive waste and the possibility of their incineration. However, ion-exchange resins (IONEX) are also used in various nuclear power plant systems for the purpose of removing specific contaminants. For example, Amberlite IRN78 with a maximum operating temperature of 60 °C is used to remove traces of chlorine contamination from the reactor cooling system and to control the boron level in the primary system of the power plant. It is also used for exhaust cleaning of the steam generator. Due to its high stability and purity, Amberlite IRN150 with a maximum operating temperature of 60 °C can also be used for cleaning the cooling water of the primary circuit. Amberlite IRN97 H with a maximum operating temperature of 120 °C is used to regulate the pH of the reactor coolant, to remove fission products and to remove Caesium-137 from water vapor.

The main function of IONEXes is the ability to bind ions contained in the liquid on their surface, which are subsequently exchanged for positively charged ions. They therefore serve as a medium for ion exchange. These are usually small porous balls with a diameter in the range of 0.3 – 1.2 mm. The porous surface provides a larger area for ion exchange. According to the size of the pores, IONEXes are divided into macroporous and gel. Gel IONEXes have a smaller pore size and are mechanically less resistant.

There are natural or synthetic IONEXes of organic or inorganic origin. Since the IONEXes used in nuclear power plants are mostly of organic origin, burning them in a dry state is not problematic. Combustion of IONEXes in a dry state is possible through fluidic combustion devices with problem-free transport of IONEXes in the form of pellets and at the same time with good air access, which is essential for high efficiency combustion. Feeding IONEXes with a high water content of approximately 40% into the furnace is problematic due to the formation of large clumps and very rapid settling of particles in a liquid transport medium. A suitable medium capable of transporting these particles is, for example, foam (liquid - gas) with sufficient thermal and temporal stability. The advantage is undemanding production directly at the place of consumption with acceptable energy requirements. Among the disadvantages is the negative impact of water on the energy balance of combustion.

II. FEEDER MODEL AND ITS COOLING PIPE VARIANTS

Figure 1 shows the basic model of the radioactive waste feeder without the cooling pipe. On the left, the feeder is shown as seen from the outside, on the right is a view of the inside of the feeder without the outer casing. The outer shell located between the face and the flange has a diameter of 202 mm. The diameter of the pipe intended for IONEXes feeding is 24 mm.

The diameter of the pipe used for the supply of liquid radioactive waste (RAW) is 16 mm. The length of both pipes is 1,500 mm.

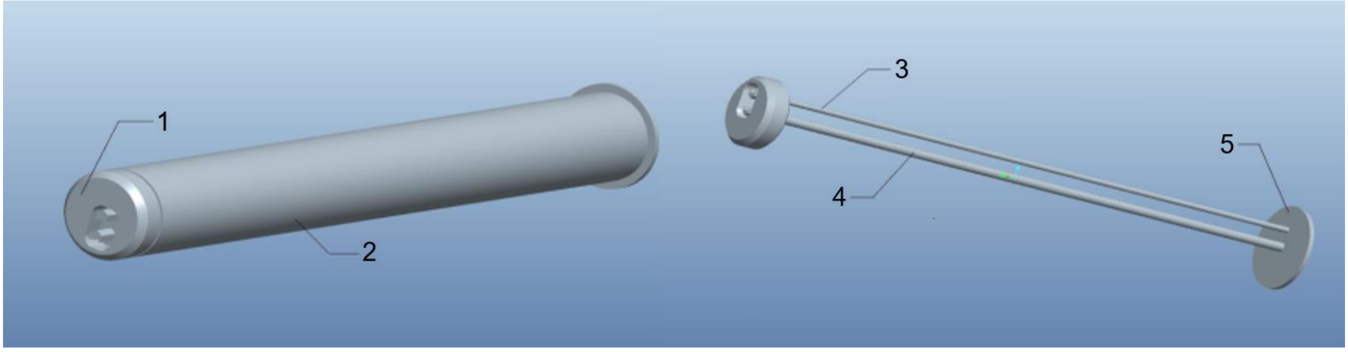

FIGURE 1: 3D model of the feeder without the cooling pipe: 1 – Front with nozzles; 2 – Outer shell; 3 – Pipe for the supply of a mixture of oil and liquid RAW; 4 – Pipe for the supply of a foam and IONEXes; 5 – Flange.

Figure 2 shows variant no. 1 of the cooling pipe. It is a reference model and at the same time the simplest design solution. The length of the cooling tube is 1400 mm, while its open end is located at a distance of 100 mm from the face of the feeder. The diameter of the cooling pipe is 50 mm. The diameter of the opening for the cooling water outlet is 40 mm.

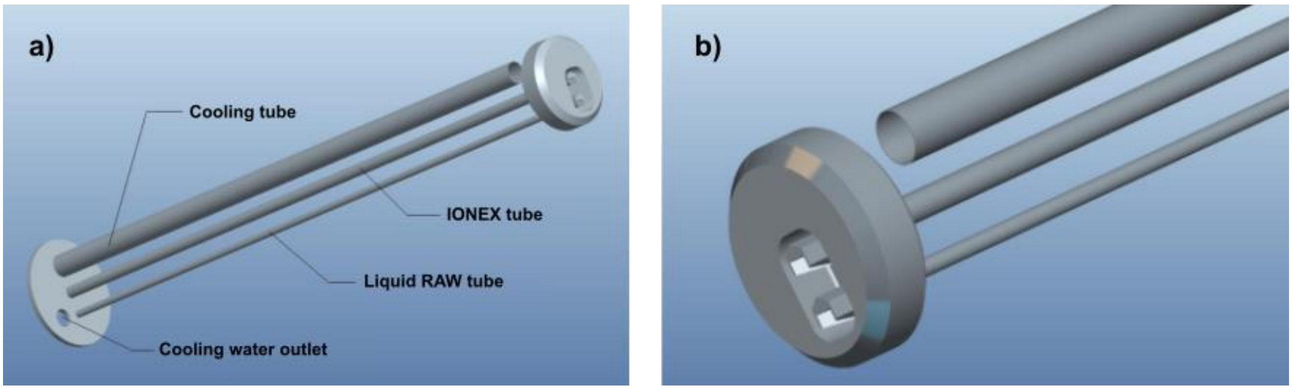

FIGURE 2: a) Variant no. 1. b) Detail of the end of the cooling pipe variant no. 1.

The cooling tube of variant no. 2 (Figure 3) has the same shape, length and diameter compared to variant no. 1. The difference lies in the creation of 9 holes with a diameter of 20 mm. The distance of the first hole from the open end of the cooling tube is 102 mm. The distance between individual holes is 70 mm. According to the assumption, the creation of holes in the cooling tube should result in the formation of a water vortex and thus the overall improvement of the cooling of the feeder shell.

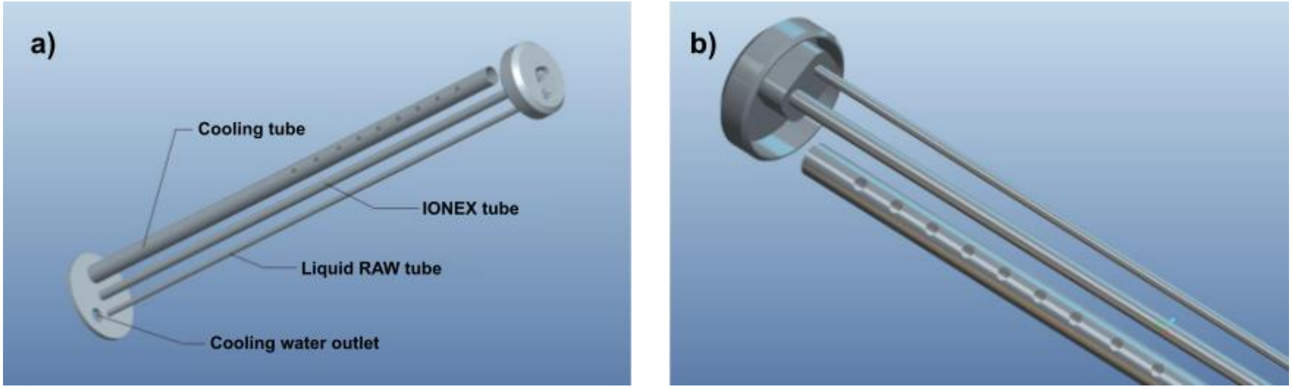

FIGURE 3: a) Variant no. 2. b) Detail of the cooling pipe variant no. 2.

The bent end of the cooling tube of variant no. 3 at an angle of 45° (Figure 4) supports the creation of a circular flow of cooling liquid at the head of the feeder. The cooling liquid should reach higher speeds in that place, which prevents excessive overheating of the liquid above the permitted temperature. This variant does not contain any holes. The diameter and length of the cooling tube is the same as for variant no. 1.

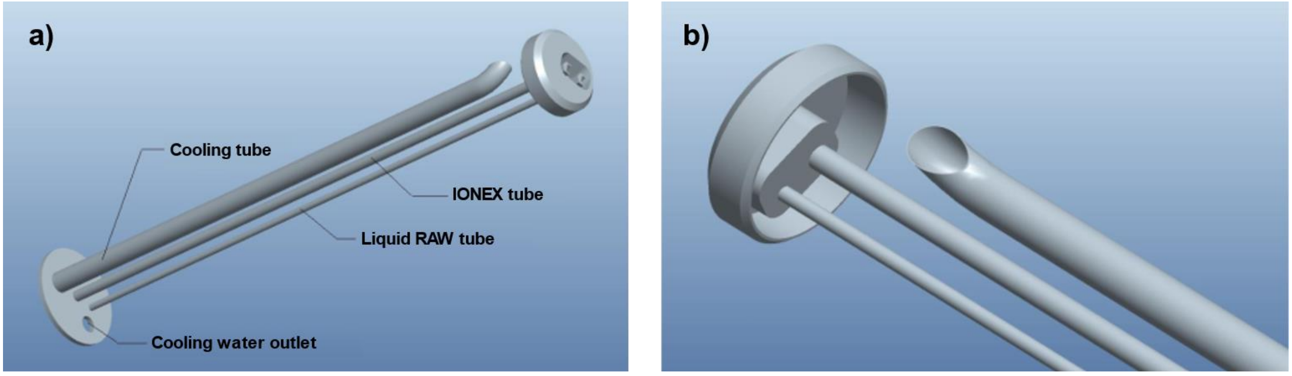

FIGURE 4: a) Variant no. 3. b) Detail of the end of the cooling pipe variant no. 3.

III. MESH GENERATION AND DEFINING SIMULATION CONDITIONS

The Tetrahedron type mesh with an element size of $5 \cdot 10^{-4}$ m is dense enough due to the dimensions of the model (Figure 5a) to provide accurate simulation results with acceptable hardware requirements. However, in order to obtain sufficiently accurate results, an additional densification of the mesh is necessary in the area of boundary layers at the boundaries of environments with different properties. In the case of the feeder model, there are 3 boundary layers. The calculation of the distance of the boundary layer from the wall was carried out in the program y+, while the distance from the wall of the shell, from the wall of the cooling tube and from the face of the feeder was determined. The individual parameters required for the calculation of the boundary layer and the subsequent resulting distances of the boundary layers are listed in Table 1.

TABLE 1
PARAMETERS FOR THE CALCULATION OF BOUNDARY LAYERS AND THE RESULTING DISTANCES OF BOUNDARY LAYERS

	Mantle boundary layer	Cooling tube boundary layer	Feeder face boundary layer
Fluid velocity ($m \cdot s^{-1}$)	2.12	0.397	2.12
Length of the boundary layer (m)	1.56	1.43	0.101
Dimensionless distance	1		
Density ($kg \cdot m^{-3}$)	0.4625		
Dynamic viscosity (Pa·s)	$34.29172 \cdot 10^{-6}$		
Distance from the wall (mm)	0.5912	2.5236	0.4085

As part of setting the environment properties, the cooling water inlet and outlet are defined in Figure 5b.

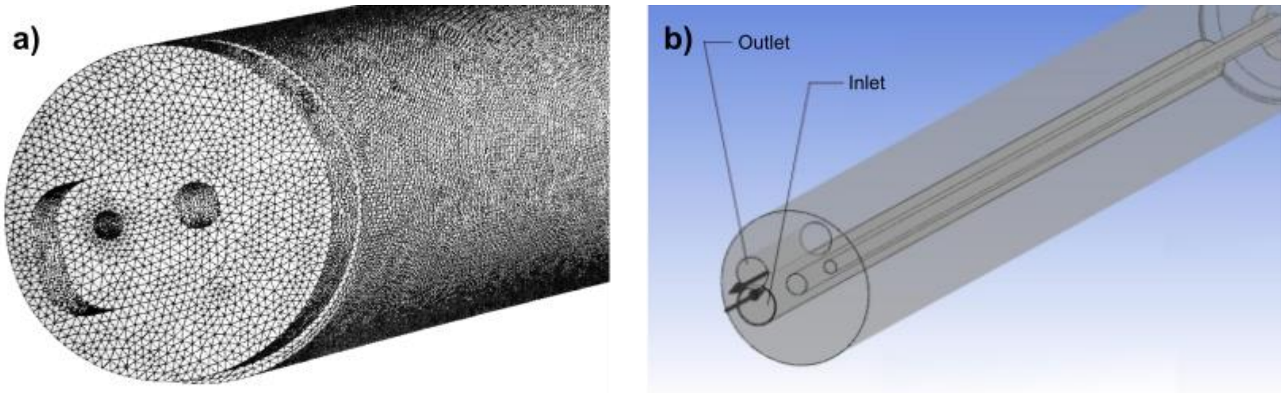

FIGURE 5: a) Mesh of the feeder model. b) Defining the coolant inlet and outlet.

Due to the changing properties and parameters of water when the temperature changes, it is not suitable for simulation purposes to use table values. More accurate simulation results can be obtained by defining water properties through equations (1-4) obtained by regression analysis based on table values:

$$\rho = 1000 - 6.714 \cdot 10^{-2} \cdot t - 3.571 \cdot 10^{-3} \cdot t^2 \tag{1}$$

where ρ is density of water (kg·m^{-3}) and t is temperature of water (°C).

$$\eta = 2.596 \cdot 10^{-4} + 11.046 \cdot 10^{6} \cdot e^{-2\left(\frac{t+1331}{395}\right)^2} \tag{2}$$

where η is dynamic viscosity of water (Pa·s).

$$c_\mathrm{p} = 4220.2 - 3.38 \cdot t + 9.111 \cdot 10^{-2} \cdot t^2 - 9.4213 \cdot 10^{-4} \cdot t^3 + 3.646 \cdot 10^{-6} \cdot t^4 \tag{3}$$

where c_p is isobaric specific heat capacity of water (J·kg^{-1}·K^{-1})

$$\lambda = 0.5565 + 2.112 \cdot 10^{-3} \cdot t - 8.661 \cdot 10^{-6} \cdot t^2 \tag{4}$$

where λ is thermal conductivity coefficient (W·m^{-1}·K^{-1})

IV. COMPARISON OF SIMULATION RESULTS

The resulting temperature layouts obtained through numerical simulation for individual variants of the feeder are shown in Figures 6 to 8. Variant no. 1 shown in Figure 6 is suitable in terms of the maximum permitted temperature of 60 °C, as the maximum temperature reached in this case is 59.2 °C. In addition, this temperature is not reached in the pipe area, but it is a surface temperature on the casing of the feeder, which does not have a direct effect on the operation of the device.

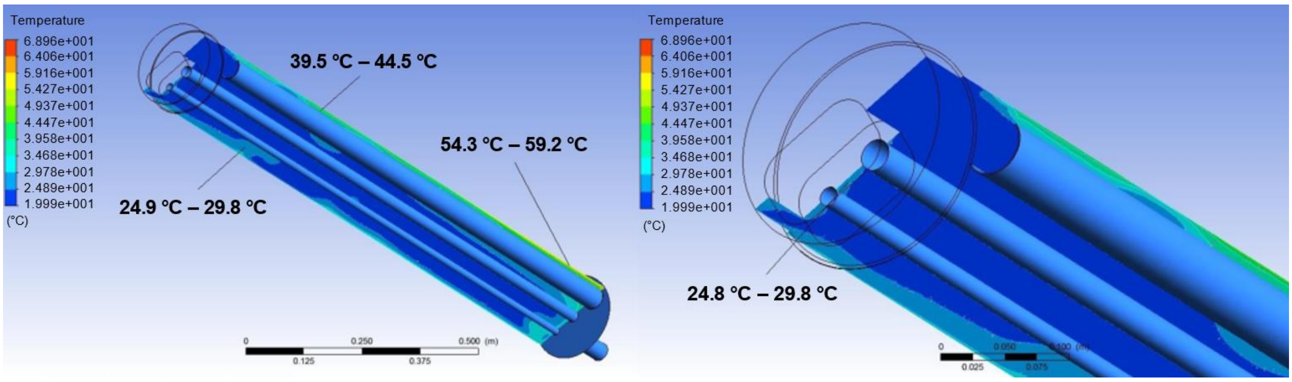

FIGURE 6: Temperature field – Variant no. 1.

Variant no. 2 in Figure 7 is also within the permitted temperature range The maximum temperature of 54.2 °C is a little lower than in the previous variant, which is again the temperature of the feeder casing.

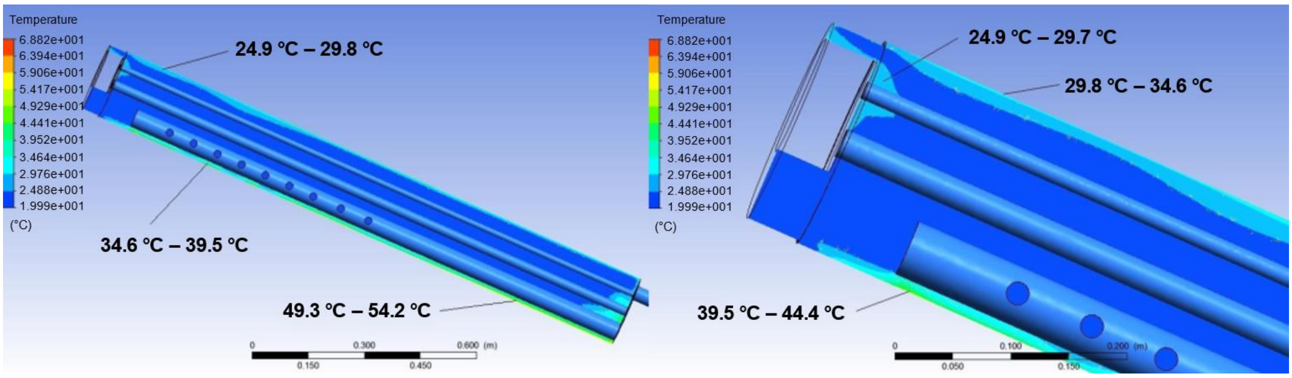

FIGURE 7: Temperature field – Variant no. 2.

The temperature field of variant no. 3 (Figure 8) reaches the lowest maximum value of 48.9 °C, so in terms of temperatures it appears to be the most suitable variant.

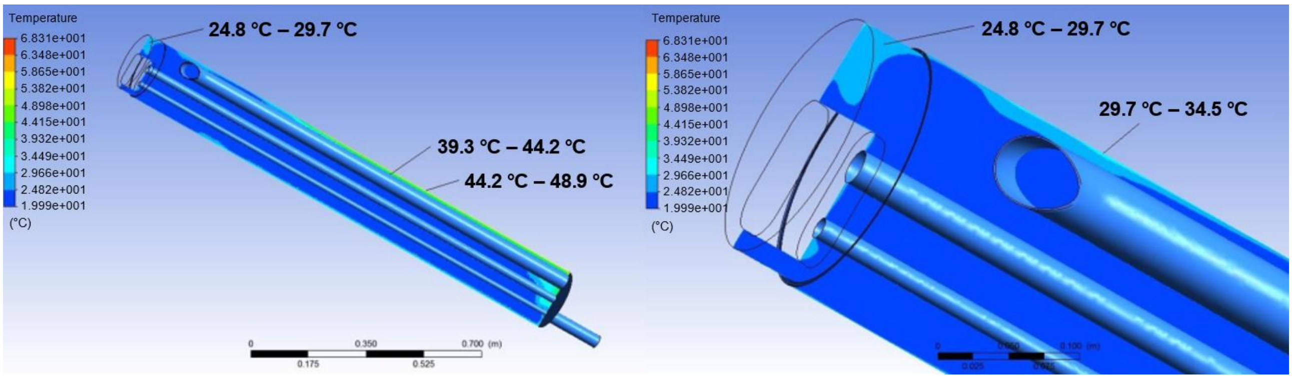

FIGURE 8: Temperature field – Variant no. 3.

The direction and speed of the cooling water flow of the individual variants are compared in Figure 9.

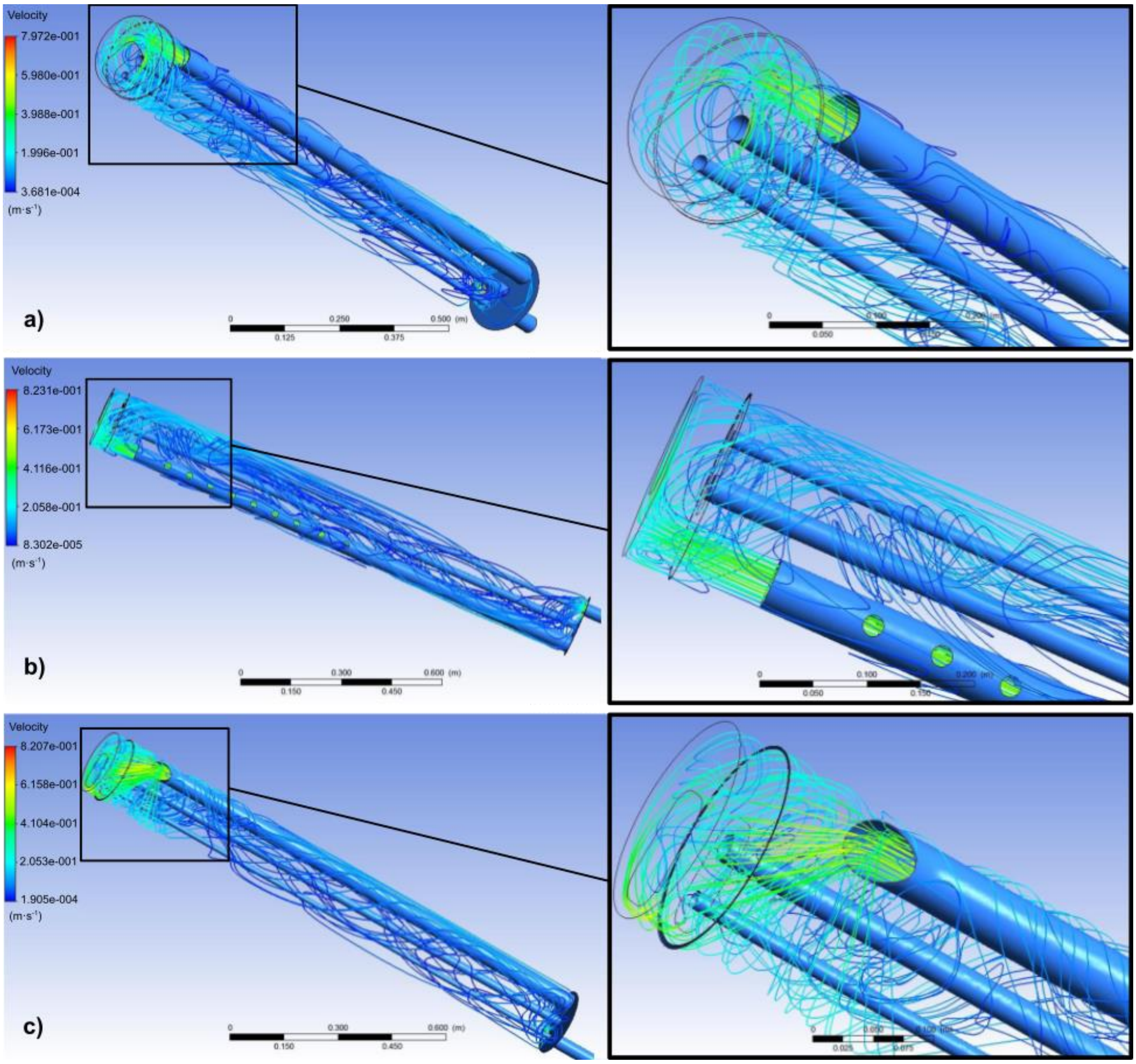

FIGURE 9: Cooling water flow. a) Variant no. 1. b) Variant no. 2. c) Variant no. 3.

When comparing variant no. 1 and variant no. 2, it is not possible to observe significant changes in the flow. The holes created in the cooling tube of variant no. 2 do not affect the nature of the flow and do not contribute to the formation of vortices. Therefore, their creation has no justification from a structural and operational point of view. On the contrary, the comparison of variant no. 1 and variant no. 3 with the bent end of the cooling tube shows a more significant change in flow in the area of the feeder face.

V. CONCLUSION

The production of electricity in nuclear power plants requires a high technical level of many devices for safe and continuous operation, including the RAW and IONEX feeders to the furnace premises. Considering the environment of the furnace with high temperatures and the limited operating temperatures of individual IONEXes, it is necessary to ensure effective cooling of these devices. When considering the mass flow of water determined by the calculation in Part I at the level of $Q_m = 0.779$ kg·s^{-1}, all 3 proposed variants are satisfactory in terms of operating temperature, while the best results in the field of cooling are provided by variant no. 3 with a curved end of the tube with a maximum temperature of 48.9 °C. Further reduction of temperatures in the feeder can be achieved, for example, by increasing the cooling water flow to the level of 1.17 kg·s^{-1}. With this increased flow, it would be possible to additionally reduce the maximum temperature by 11 °C.

ACKNOWLEDGEMENTS

This paper was written with financial support from the VEGA granting agency within the projects no. 1/0224/23 and no. 1/0532/22, from the KEGA granting agency within the project no. 012TUKE-4/2022 and with financial support from the APVV granting agency within the projects no. APVV-15-0202, no. APVV-20-0205 and no. APVV-21-0274.

REFERENCES

[1] G. Darmograi, B. Prelot, A. Geneste, L.-Ch. De Menoryal, J. Zajac, "Removal of three anionic orange-type dyes and Cr(VI) oxyanion from aqueous solutions onto strongly basic anion-exchange resin. The effect of single-component and competitive adsorption". In: *Colloids and Surfaces A: Physicochemical and Engineering Aspects*, 2016. Volume 508, pages 240-250, ISSN 0927-7757. DOI: < https://doi.org/10.1016/j.colsurfa.2016.08.063>

[2] M. Sillanpää, M. Shestakova, "Chapter 3 - Emerging and Combined Electrochemical Methods". In: *Electrochemical Water Treatment Methods,* 2017. Butterworth-Heinemann. Pages 131-225. ISBN 9780128114629. DOI: <https://doi.org/10.1016/B978-0-12-811462-9.00003-7>

[3] Evoqua. "Ion Exchange Resins for Nuclear Power Plants" [online]. Available at: <https://www.evoqua.com/en/markets/applications/ion-exchange-resins-for-nuclear-power-plants/> [cit. 10-10-2023]

[4] J. Irving, "WATER TREATMENT | Overview: Ion Exchange". In: *Encyclopedia of Separation Science*. Academic Press, 2000. Pages 4469-4477, ISBN 9780122267703. DOI: <https://doi.org/10.1016/B0-12-226770-2/02031-7>

[5] S. Lecheler, "Computational Fluid Dynamics: Getting Started Quickly With ANSYS CFX 18 Through Simple Examples". 2022. Springer, 1st edition. 220 pages. ISBN 978-3658384524.

[6] T. Brestovič, N. Jasminská, "Numerické metódy a modelovanie v energetike", 2015. Strojnícka fakulta Technickej univerzity v Košiciach. 113 pages. ISBN 978-80-553-2067-0.